Gravitational quasinormal modes of static Einstein-Gauss-Bonnet anti-de Sitter black holes[*]

Hong Ma(马洪)   Jin Li(李瑾)[1)]

Department of Physics, Chongqing University, Chongqing 401331, China

Abstract: In this paper, we describe quasinormal modes (QNMs) for gravitational perturbations of Einstein-Gauss-Bonnet black holes (BHs) in higher dimensional spacetimes, and derive the corresponding parameters of such black holes in three types of spacetime (flat, de Sitter (dS) and anti-de Sitter (AdS)). Our attention is concentrated on discussing the (in)stability of Einstein-Gauss-Bonnet AdS BHs through the temporal evolution of all types of gravitational perturbation fields (tensor, vector and scalar). It is concluded that the potential functions in vector and scalar gravitational perturbations have negative regions, which suppress quasinormal ringing. Furthermore, the influences of the Gauss-Bonnet coupling parameter α, the number of dimensions n and the angular momentum quantum number l on the Einstein-Gauss-Bonnet AdS BHs quasinormal spectrum are analyzed. The QNM frequencies have greater oscillation and lower damping rate with the growth of α. This indicates that QNM frequencies become increasingly unstable with large α. Meanwhile, the dynamic evolutions of the perturbation field are compliant with the results of computation from the Horowitz and Hubeny method. Because the number of extra dimensions is connected with the string scale, the relationship between α and properties of Einstein-Gauss-Bonnet AdS BHs might be beneficial for the exploitation of string theory and extra-dimensional brane worlds.

Keywords: Einstein-Gauss-Bonnet AdS BHs, gravitational perturbation, quasinormal modes (QNMs)

PACS: 04.70.Bw, 04.62.+v, 04.70.-s   **DOI:** 10.1088/1674-1137/42/4/045101

1   Introduction

In recent years, discussion of the properties and behavior of gravity in higher dimensions has become a significant issue in gravity theories. Of these, Einstein-Gauss-Bonnet (EGB) theory [1–3] is meaningful to study since it is essential for our understanding of quantum gravity [4], extra dimensional brane-world scenarios [5], and string theory [6, 7]. EGB theory is seen as a promising candidate for an effective model of gravity from the low energy limits of string theory [8].

EGB theory indicates the presence of a coupling parameter α in the Lagrangian squared in curvature, except for the ordinary Einstein-Hilbert term [9] in higher dimensional spacetimes. In 4-dimensional spacetimes the Gauss-Bonnet coupling parameter α is a topological invariant (it is basically a total derivative), so it is trivial [10, 11]. Accordingly, BHs in EGB theory [12] have received widespread attention, because of the possibility that they might be produced at the LHC [13]. A spherically symmetric solution representing a static BH has been derived by Boulware et al. [14] and Wheeler [15]

in EGB gravity. The evolution of gravitational perturbations of D-dimensional BHs has been analyzed by Ishibashi and Kodama in pure Einstein theory. Subsequently, Konoplya considered the scalar field QNMs of EGB BHs in asymptotically flat and dS/AdS spacetimes [16, 17], and the stability of EGB BHs [18–21]. Meanwhile, Dotti and Gleiser [22, 23] separated and decoupled the EGB perturbed equations, which reduce to a waveform with some effective potentials. However, EGB theory is extremely difficult. Even if an effective potential equation is obtained, the S-deformations still cannot conveniently remove the negative regions in the potentials, since one needs an ansatz that converts the potential to a positive definite form [24]. Consequently, our purpose in this article is to investigate the stability of EGB BHs by analyzing the dynamic evolution of all types of gravitational perturbations field (tensor, vector and scalar) in higher dimensional anti-de Sitter (AdS) spacetimes.

There are three different stages in the evolution of a BH perturbed by external fields. First is the initial wave bursts phase. The second stage corresponds to

damp oscillations with complex frequencies (these are unconventional oscillations, which are called quasinormal modes [25]). The final stage is called the late-time tail. At the stage when a black hole decays with perturbations, the perturbed BH is transformed into an unperturbed one which is dominated by QNMs [26]. The eigenfrequencies of QNMs are complex. The real part describes the actual frequency of the oscillation rate and the imaginary part represents the damping rate of the frequency [27]. QNMs have been used as a powerful tool to reveal the intrinsic properties of BHs, because the modes characterize the geometry and are independent from extrinsic properties and their geometry [28]. These frequencies from a BH spectrum are responsive to external perturbations. If a BH becomes unstable, a small perturbation must expand with time [29]. In other words, the semi-classical quantum spectral information of the interior region of a BH will probably be given by QNMs [30–33]. So, QNMs provide an incentive to analyze the interior of Einstein-Gauss-Bonnet BHs.

Recently there have been four confirmed gravitational wave events from the merger of binary BHs detected by Advanced LIGO, where QNMs also appeared [34–37]. The results show that the gravitational wave (GW) signals comply with Einstein's theory of gravity. However, the evolution of binary BHs simulated by the LIGO and VIRGO collaborations has forecast that the experimental precision available at present might satisfy the requirements for testing modified theories of gravity [36]. In other words, some non-negligible parameters of indeterminacy in the range of the BHs show that the window for alternative theories of gravity is opened [38]. Therefore, EGB gravity could realistically be confirmed through corresponding GW observations.

Higher dimensional BHs are considered under AdS/CFT correspondence [39], where string theory is equivalent to a conformal field theory (CFT) with one less dimension in AdS spacetime [40]. In AdS BHs, AdS/CFT is connected to the QNM frequencies of the a test field and the decay rates in the CFT [41]. In this framework, a BH with a characteristic temperature fixed by the Hawking effect should be consistent with CFT at finite temperature. The temporal evolution of perturbation thermal state regression thermal equilibrium is described by QNMs [42]. Therefore, as for AdS BHs in Einstein's theory of gravity, the QNMs of large Gauss-Bonnet-AdS BHs can also be derived by a holographic interpretation in CFT [43]. Many studies on AdS BHs have been presented in Refs. [44–50].

The purpose of this paper is to show a numerical analysis of the evolution of gravitational perturbations of higher dimensional Einstein-Gauss-Bonnet AdS BHs. The properties of Einstein-Gauss-Bonnet BHs in asymp-

totically flat, de Sitter (dS), and AdS spacetimes are first discussed. The emphasis is placed on studying AdS spacetime. What will happen to the QNM spectrum of an Einstein-Gauss-Bonnet BH if the Gauss-Bonnet coupling parameter α is varied is taken into consideration. We also study Einstein-Gauss-Bonnet AdS BH QNMs with different dimensionalities of spacetime n and different multipole numbers l. The results indicate that the quasinormal behavior crucially relies on α and n. Thus, α leads to increase in oscillation frequency and decrease of the decay rate in AdS spacetimes.

In addition, the potentials for vector and scalar perturbations have negative regions, where quasinormal ringing of the behavior with exponential tail may be restrained, which does not cause instability. However, when α increases to a certain critical value, the QNMs in Einstein-Gauss-Bonnet AdS spacetime become unstable.

The paper is structured as follows. We review the Einstein-Gauss-Bonnet BH solutions from second-order Lovelock gravity, discussing properties in three different spacetimes (flat, dS and AdS), in Section 2. Later we focus on the Einstein-Gauss-Bonnet AdS spacetimes. In Section 3, the wave equations describing all types of gravitational perturbations and the properties of the master equations are calculated. Section 4 mainly analyzes the QNMs. In Section 4.1, the dynamical evolution of the gravitational perturbation fields in Einstein-Gauss-Bonnet AdS spacetime is analyzed by the finite difference method [51]. In Section 4.2, QNMs for Einstein-Gauss-Bonnet AdS BHs are calculated by utilizing the method proposed by Gary T. Horowitz and Veronika E. Hubeny [52, 53]. The key results and some remarks are summarized in Section 5.

2   Spherically symmetric static Einstein-Gauss-Bonnet BH solutions

Lovelock gravity is an extension of Einstein theory in a $(n+1)$-dimensional manifold $\mathcal{M}$ [54]. The Lanczos-Lovelock action has the following form [55],

$$I_G = \frac{1}{16\pi} \int \mathrm{d}^{n+1}x \sqrt{-g} \sum_{p=0}^{[n/2]} \alpha_p \mathcal{L}_p, \qquad (1)$$

where α_p is the Lovelock coefficient, $[n/2]$ indicates the integer part, and $\mathcal{L}_p$ is the Euler density [54], which is defined by

$$\mathcal{L}_p = \frac{1}{2^p} \delta_{\rho_1\sigma_1\cdots\rho_p\sigma_p}^{\mu_1\nu_1\cdots\mu_p\nu_p} R_{\mu_1\nu_1}{}^{\rho_1\sigma_1} \cdots R_{\mu_p\nu_p}{}^{\rho_p\sigma_p}. \qquad (2)$$

Here, $R_{\mu\nu}{}^{\rho\sigma}$ is the D-dimensional Riemann tensor and $\delta_{\rho_1\sigma_1\cdots\rho_p\sigma_p}^{\mu_1\nu_1\cdots\mu_p\nu_p}$ is the Kronecker delta.

In general, it is more convenient to calculate the equations of motion in the Hamiltonian formulation [55]. For the purposes of discussion, we have chosen a decomposition of spacetime into time and space, which allows discernment of the dynamic properties of general relativity [56]. Furthermore, the spatial metric h_{ij} replaces the spacetime metric $g^{\mu\nu}$ as the dynamical variable. Here h_{ij} stands for the induced metric, and its conjugate momentum can be expressed as [57]

$$\pi^i_{\ j} = -\frac{1}{4}\sqrt{-g}\sum_{p=0}^{n}\frac{\alpha_p}{2^p}\sum_{s=0}^{p-1}\frac{(-4)^{p-s}}{s![2(p-s)-1]!!}\delta^{i_1\ldots i_{2p-1}i}_{[j_1\ldots j_{2p-1}j}$$
$$\times \hat{R}^{j_1j_2}_{\ \ \ i_1i_2}\cdots \hat{R}^{j_{2s-1}j_{2s}}_{\ \ \ \ \ i_{2s-1}i_{2s}}K^{j_{2s+1}}_{\ \ \ i_{2s+1}}\cdots K^{j_{2p-1}}_{\ \ \ i_{2p-1}},$$
(3)

where $\hat{R}_{ijkl}$ is the intrinsic component of the curvature tensor of the boundary Σ_t, and $K^i_{\ j}$ is the extrinsic curvature, expressed as [57]:

$$K_{ij} = \frac{1}{2}N^{-1}(\dot{h}_{ij} - D_j N_i - D_i N_j),$$
(4)

Here $N = (-g^{00})^{-1/2}$ and $N^i = h^{ij}g_{0\mu}$ represent the 'lapse function' and 'shift vectors' respectively. In the ADM (Arnowitt-Deser-Misner) spacetime decomposition, D_i is defined as the covariant derivative connected with h_{ij} [55]. $g_{0\mu}$ is the Lagrange multiplier linked to surface deformation and

$$\mathcal{H} = -\sqrt{h}\sum_p \alpha_p \frac{1}{2^p}\delta^{i_1\ldots i_{2p}}_{j_1\ldots j_{2p}}R^{j_1j_2}_{\ \ \ i_1i_2}\cdots R^{j_{2p-1}j_{2p}}_{\ \ \ \ \ i_{2p-1}i_{2p}},$$
(5)

where $\mathcal{H}_i = -2\pi^j_{\ i|j}$, and $R^{ij}_{\ \ kl}$ describes the spatial components curvature tensor. $R^{ij}_{\ \ kl}$ is given by the Gauss–Codacci equation [58],

$$R_{ijkl} = \hat{R}_{ijkl} + K_{ik}K_{jl} - K_{il}K_{jk}.$$
(6)

So the Hamiltonian formulation of the action Eq. (1) becomes [56]

$$I_G = \frac{1}{16\pi}\int \mathrm{d}t\mathrm{d}^n x(\pi^{ij}\dot{h}_{ij} - N\mathcal{H} - N^i\mathcal{H}_i) + B,$$
(7)

where B is a surface term. Based on the relationship between the Gauss-Codacci relation Eq. (6) and the extrinsic curvature K_{ij} [55], the generator of surface deformation Eq. (5) can be simplified to be $\mathcal{H} = \sum \alpha_p\mathcal{L}_p$. Moreover, due to the second order Lovelock gravity, we focus on the first three terms of the Hamiltonian action Eq. (7), which becomes

$$I_G = \frac{1}{16\pi}\int \mathrm{d}t\mathrm{d}^n x N\sqrt{h}[\mathcal{L}_0 + \mathcal{L}_1 + \alpha_2\mathcal{L}_2] + B,$$
(8)

where

$$\mathcal{L}_0 = -2\Lambda,$$
(9)
$$\mathcal{L}_1 = R,$$
(10)
$$\mathcal{L}_2 = R_{ijkl}R^{ijkl} - 4R_{ij}R^{ij} + R^2.$$
(11)

$\Lambda = -n(n-1)/2l^2$ represents the cosmological constant in AdS spacetimes, and α_2 is the Gauss-Bonnet coupling parameter. $\mathcal{L}_1$ and $\mathcal{L}_2$ describe the Einstein-Hilbert Lagrangian and the second order Lovelock Lagrangian respectively.

Consider the metric of static vacuum solution of the EGB equation,

$$\mathrm{d}s^2 = -f(r)\mathrm{d}t^2 + \frac{1}{f(r)}\mathrm{d}r^2 + r^2\mathrm{d}\Omega_n^2,$$
(12)

where

$$f(r) = \kappa - r^2\psi(r),$$
(13)

where $\psi(r)$ satisfies [18]

$$W[\psi] \equiv \frac{\alpha n(n-1)(n-2)}{4}\psi^2 + \frac{n}{2}\psi - \frac{\Lambda}{n+1} = \frac{\mu}{r^{n+1}},$$
(14)

and $\mathrm{d}\Omega_n^2$ represents the $(n=D–2)$-dimensional hypersurface with $\kappa = \pm 1, 0$. μ is proportional to the mass of the BH, which is a positive constant.

There are two solutions can be obtained from the quadratic equation, given by

$$\psi(r) = \frac{1}{\alpha(n-1)(n-2)}$$
$$\times\left(\epsilon\sqrt{1 + \frac{4\alpha(n-1)(n-2)}{n}\left(\frac{\mu}{r^{n+1}} + \frac{\Lambda}{n+1}\right)} - 1\right),$$
(15)

where $\epsilon = \pm 1$. The asymptotic anti-de Sitter solutions are studied in this paper (i.e., $\epsilon = 1$ and $\Lambda < 0$). Then we can infer the same properties of the metric as Ref. [59].

In order to reduce the relative error in Eq.(15), its alternative equivalent form is used (for $\epsilon = 1$) [18]

$$\psi(r) = \frac{4\left(\dfrac{\mu}{r^{n+1}} + \dfrac{\Lambda}{n+1}\right)}{n + \sqrt{n^2 + 4\alpha n(n-1)(n-2)\left(\dfrac{\mu}{r^{n+1}} + \dfrac{\Lambda}{n+1}\right)}}.$$
(16)

For $\kappa = 1$, an Einstein-Gauss-Bonnet BH solution can be obtained as

$$f(r) = 1 - \frac{4r^2\left(\dfrac{\mu}{r^{n+1}} + \dfrac{\Lambda}{n+1}\right)}{n + \sqrt{n^2 + 4\alpha n(n-1)(n-2)\left(\dfrac{\mu}{r^{n+1}} + \dfrac{\Lambda}{n+1}\right)}},$$
(17)

where α is the Gauss-Bonnet coupling parameter and $\alpha \to 0$ EGB gravity leads to the Schwarzschild-Tangherlini spacetime from a higher dimensional solution [60].

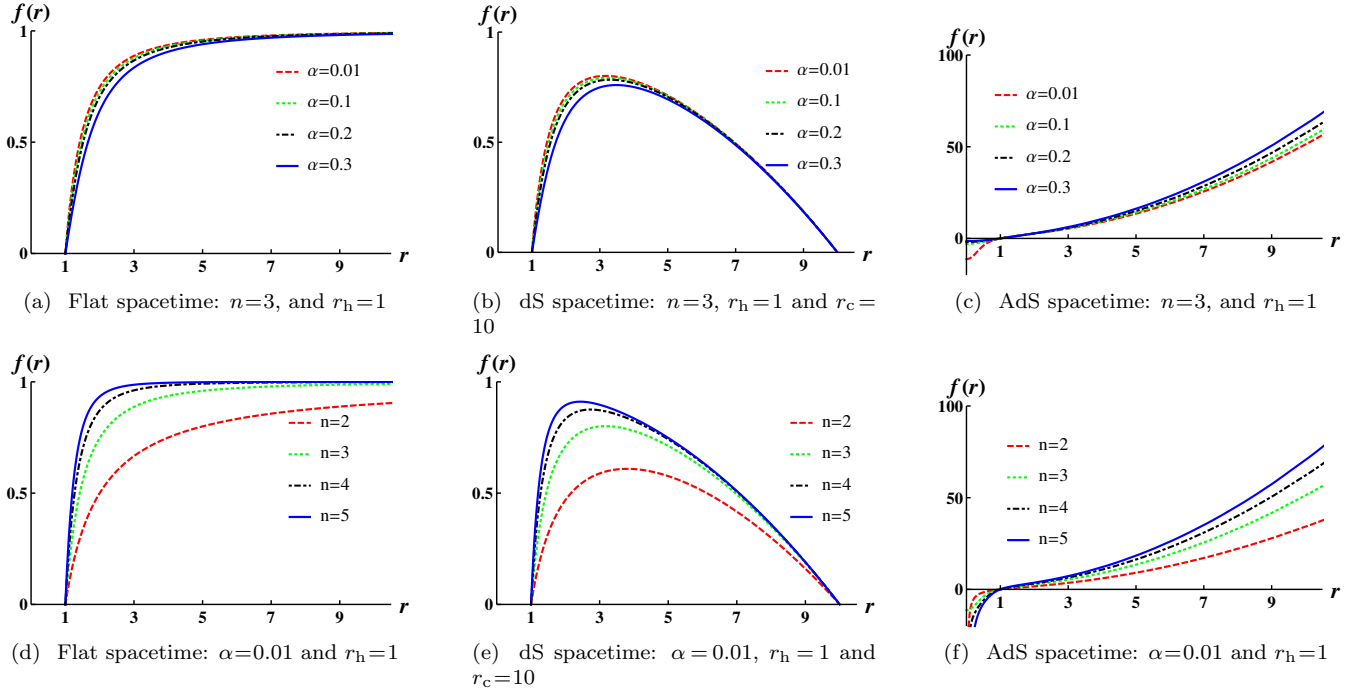$$f(r) = \kappa - \frac{2r^2}{n}\left(\frac{\mu}{r^{n+1}} + \frac{\Lambda}{n+1}\right).$$
(18)

(a) Flat spacetime: $n=3$, and $r_{\rm h}=1$

(b) dS spacetime: $n=3$, $r_{\rm h}=1$ and $r_{\rm c}=10$

(c) AdS spacetime: $n=3$, and $r_{\rm h}=1$

(d) Flat spacetime: $\alpha=0.01$ and $r_{\rm h}=1$

(e) dS spacetime: $\alpha=0.01$, $r_{\rm h}=1$ and $r_{\rm c}=10$

(f) AdS spacetime: $\alpha=0.01$ and $r_{\rm h}=1$

Fig. 1.   (color online) The structures of the Einstein-Gauss-Bonnet BH's metric function $f(r)$ with different values of α ((a)-(c), $n=3$) and n ((d) - (f), $\alpha=0.01$): (a) and (d) show asymptotically flat spacetimes with $r_{\rm h}=1$; (b) and (e) show de Sitter spacetimes with $r_{\rm h}=1$ and $r_{\rm c}=10$; and (c) and (f) show anti-de Sitter spacetimes with $r_{\rm h}=1$.

According to the event horizon radius $r_{\rm h}$, we can express parametrization of the BH mass μ as:

$$\mu=\frac{nr_{\rm h}^{n-1}}{4}\left(2+\frac{\alpha(n-2)(n-1)}{r_{\rm h}^2}-\frac{4\Lambda r_{\rm h}^2}{n(n+1)}\right). \qquad (19)$$

Here, we investigate the effect of Λ on Einstein-Gauss-Bonnet BH spacetime. The parameters $\Lambda=0$, $\Lambda>0$, $\Lambda<0$ in Einstein-Gauss-Bonnet BH spacetime can be classified into asymptotically flat, dS, and AdS spacetime respectively.

(1) For asymptotically flat spacetime:

$$\Lambda=0, \qquad (20)$$

Here $r\to\infty$, $f(r)\to1$, and the spacetime is asymptotically flat. We note when $\alpha\to0$ in 4-dimensional ($n=2$) spacetime, Eq.(17) returns to Schwarzschild flat spacetime.

(2) For the de Sitter spacetime [18]:

$$\Lambda=\frac{n(n+1)}{2}\left(\frac{r_{\rm c}^{n-1}-r_{\rm h}^{n-1}}{r_{\rm c}^{n+1}-r_{\rm h}^{n+1}}+\frac{\alpha(n-1)(n-2)}{2}\frac{r_{\rm c}^{n-3}-r_{\rm h}^{n-3}}{r_{\rm c}^{n+1}-r_{\rm h}^{n+1}}\right), \qquad (21)$$

where $r_{\rm c}$ and $r_{\rm h}$ are the cosmological horizon and the event horizon respectively. In dS spacetimes, the condition $r_{\rm c}>r_{\rm h}$ limits the span of the spatial coordinate [61]. We note when $\alpha\to0$ in 4-dimensional ($n=2$) spacetime, Eq.(17) returns to Schwarzschild dS spacetime.

(3) For anti-de Sitter spacetime:

$$\Lambda=-\frac{n(n-1)}{2r_{\rm h}^2}, \qquad (22)$$

where $r_{\rm h}$ is the event horizon of AdS spacetime. For AdS spacetime, we choose $f(r)\to r^2$ with $r\to\infty$ without loss of generality. We note that when $\alpha\to0$ in 4-dimensional ($n=2$) spacetime, Eq.(17) becomes Schwarzschild AdS spacetime. In this paper, attention is concentrated on analyzing the gravitational perturbations of Einstein-Gauss-Bonnet in AdS spacetime.

Generally, the cosmological constant Λ and the mass μ can be described according to α, n, $r_{\rm h}$ and $r_{\rm c}$. Therefore, Fig. 1 shows that α, n, $r_{\rm h}$ and $r_{\rm c}$ can determine the structure of Einstein-Gauss-Bonnet BH spacetime. For the asymptotically flat spacetime, with larger α, the spacetime approaches flatness more slowly, while the spacetime goes flat at infinity more quickly with increasing n. For dS spacetime, it is bounded by two horizons $r_{\rm h}<r<r_{\rm c}$. The spacetime becomes less curved with the increase of α (with n fixed), but more curved with the increase of n (with α). However, as α and n increase, AdS spacetime approaches infinity more quickly.

3   Gravitational perturbations

Considering the first order gravitational perturbations of static EGB gravity, the metric functions can be

represented as

$$g_{\mu\nu}=\bar{g}_{\mu\nu}+h_{\mu\nu}, \qquad (23)$$

where $h_{\mu\nu}$ is a small perturbation, and $\bar{g}_{\mu\nu}$ is the background metric. Correspondingly, the inverse of the metric perturbation can be expressed as:

$$g^{\mu\nu}=\bar{g}^{\mu\nu}-h^{\mu\nu}. \qquad (24)$$

According to Eq.(23) and Eq.(24), the perturbation of the Christoffel symbol due to the metric perturbation is:

$$\delta\Gamma_{\mu\nu}^{\beta}=\frac{1}{2}\bar{g}^{\beta\alpha}(h_{\alpha\nu;\mu}+h_{\alpha\mu;\nu}-h_{\mu\nu;\alpha}), \qquad (25)$$

where we use ';' to denote a covariant derivative. We then get the perturbed Ricci tensor as:

$$\delta R_{\mu\nu}=\delta\Gamma_{\mu\alpha;\nu}^{\alpha}-\delta\Gamma_{\mu\nu;\alpha}^{\alpha}. \qquad (26)$$

Variations of the Einstein-Gauss-Bonnet equations for vacuum solutions are derived as follows [18],

$$\delta G_{\mu}{}^{\nu}=\Lambda\delta G_{(0)\mu}{}^{\nu}+\delta G_{(1)\mu}{}^{\nu}+\alpha\delta G_{(2)\mu}{}^{\nu}=0, \qquad (27)$$

where

$$G_{(0)\mu}{}^{\nu} = \delta_{\mu}^{\nu}, \qquad (28)$$

$$G_{(1)\mu}{}^{\nu} = R_{\mu}{}^{\nu}-\frac{1}{2}\delta_{\mu}^{\nu}R \qquad (29)$$

and

$$G_{(2)\mu}{}^{\nu} = R_{\lambda\mu}{}^{\delta\sigma}R_{\delta\sigma}{}^{\lambda\nu}-2R_{\delta}{}^{\lambda}R_{\lambda\mu}{}^{\delta\nu}-2R_{\mu}{}^{\lambda}R_{\lambda}{}^{\nu}+RR_{\mu}{}^{\nu}$$
$$-\frac{1}{4}\delta_{\mu}^{\nu}\left(R_{\lambda\delta}{}^{\sigma\rho}R_{\sigma\rho}{}^{\lambda\delta}-4R_{\lambda}{}^{\delta}R_{\delta}{}^{\lambda}+R^2\right). \qquad (30)$$

The contribution of parameter α to the Einstein tensor can be found. It is shown in Refs. [22, 23] that the perturbations of an Einstein-Gauss-Bonnet AdS BH can be decomposed into an angular part [62] and a radial part. The master differential equations can be expressed as

$$\left(\frac{\partial^2}{\partial t^2}-\frac{\partial^2}{\partial r_*^2}+V_i(r_*)\right)\Psi(t,r_*)=0, \qquad (31)$$

where i represents tensor, vector and scalar perturbations respectively. A tortoise coordinate r_* is given by,

$$\mathrm{d}r_*\equiv\frac{\mathrm{d}r}{f(r)}=\frac{\mathrm{d}r}{1-r^2\psi(r)}. \qquad (32)$$

The effective potentials in $V_t(r)$, $V_v(r)$, and $V_s(r)$ are given respectively as [62]

$$V_t(r) = \frac{\ell(\ell+n-1)f(r)T''(r)}{(n-2)rT'(r)}+\frac{1}{R(r)}\frac{\mathrm{d}^2}{\mathrm{d}r_*^2}\bigg(R(r)\bigg), \quad (33)$$

$$V_v(r) = \frac{(\ell-1)(\ell+n)f(r)T'(r)}{(n-1)rT(r)}+R(r)\frac{\mathrm{d}^2}{\mathrm{d}r_*^2}\bigg(\frac{1}{R(r)}\bigg),$$

$$V_s(r) = \frac{2\ell(\ell+n-1)}{nr^2B(r)}\frac{\mathrm{d}}{\mathrm{d}r_*}\bigg(rB(r)\bigg)+B(r)\frac{\mathrm{d}^2}{\mathrm{d}r_*^2}\bigg(\frac{1}{B(r)}\bigg),$$

where $\ell=2,3,4,\dots$ stands for the multipole number and

$$T(r)=r^{n-1}\frac{\mathrm{d}W}{\mathrm{d}\psi} = \frac{nr^{n-1}}{2}\bigg(1+\alpha(n-1)(n-2)\psi(r)\bigg),$$

$$R(r)=r\sqrt{T'(r)}, \quad B(r)=\frac{2(\ell-1)(\ell+n)-nr^3\psi'(r)}{r\sqrt{T'(r)}}T(r).$$

Equation (33) can be used to discuss how parameters such as α, n and l impact the effective potential in AdS spacetime. The form of the effective potential in AdS spacetime is quite different from that in flat and dS spacetime. The potential function in AdS spacetime is mostly a convex function. Potentials of gravitational perturbations are given in Fig. 2.

From Fig.2(a) - (c), we can see that with the increase of the α ($\alpha\leq0.3$), the potentials in all the cases are enhanced. As α increases, some negative regions emerge in the vector and scalar perturbation. Then we can find that when α increases to certain critical value ($\alpha=0.45$, 0.5, 0.35), the potentials are different. Therefore, it is necessary to further consider the temporal evolution of higher dimensional AdS Einstein-Gauss-Bonnet BHs and analyze the (in)stability of the BHs in each type of perturbation.

For the potentials with tensor and vector perturbations, the Fig. 2(d) - (f) shows us that as the dimension number n increases, the potential values also increases. Figure 2(g) - (i) shows that the potential increases with the growth of l. Effective potentials are positive definite beyond the event horizon in the tensor and vector perturbations. However, the features of the potential for scalar perturbations is different from the other types. The scalar perturbations have a negative region. From Fig. 2(f), the increase of n makes the negative gap appear. From Fig. 2(i), the increase of l leads to the peak value of the potential increasing. The potential is not positive definite any more for scalar perturbations.

4 Numerical calculation of the QNM frequencies for Einstein-Gauss-Bonnet Anti-de Sitter BHs

QNMs reflect the intrinsic properties of the black holes. In order to obtain the QNM frequencies of black holes, boundary conditions should be imposed on the master equation. At the horizon there are only ingoing waves, and at infinity there are only purely outgoing waves, which mean discrete sets of complex frequency ω meeting these requirements [28]. The study of the potential function in Einstein-Gauss-Bonnet AdS spacetime in Section 3 showed that $V(r) \to \infty$ at infinity. Therefore, a number of numerical methods are ineffective with $V(r) \to \infty$ at infinity, for instance the WKB method [63, 64], Pöschl-Teller approximation [65], integral phase method [66] and Continuous Fraction
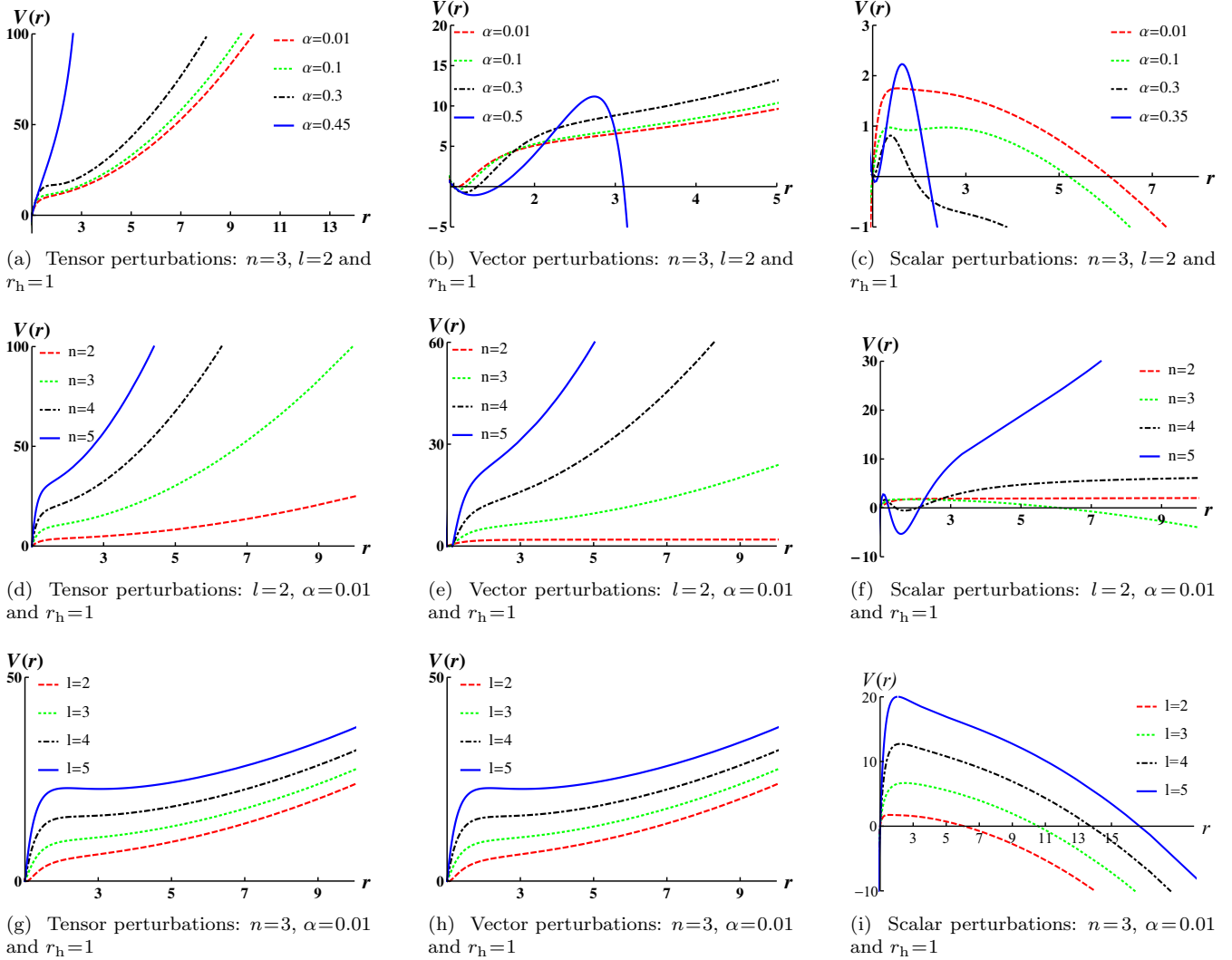
Fig. 2.   (color online) The potential of gravitational perturbations in Einstein-Gauss-Bonnet AdS spacetime ($\Lambda = -\frac{n(n-1)}{2r_{\rm h}^2}$ and $r_{\rm h}=1$) with different values of α, n, and l. (a), (d) and (g) are tensor perturbations; (b), (e) and (h) are vector perturbations; and (c), (f) and (i) are scalar perturbations.

method [67].   However, to overcome this issue, Gary T. Horowitz and Veronika E. Hubeny [52, 53] have discussed the boundary condition at infinity in AdS spacetimes. Moreover, the finite difference method [51, 52] can also be employed in AdS spacetime to study QNMs. Therefore, in this section, we will firstly use the finite difference method to solve the dynamics evolution of the gravitational perturbation fields and analyze the stability of Einstein-Gauss-Bonnet BHs in AdS spacetime. Secondly, the QNM frequencies varying with dimension n and Gauss-Bonnet coupling parameter α are calculated by the Horowitz and Hobeny method.

4.1   Dynamics evolution of the gravitational perturbations

Using the finite difference method [51, 52], we study the ringing of Einstein-Gauss-Bonnet BHs in AdS space-

time, which can directly reflect the (in)stability of the BH [68] with all the frequencies in the temporal evolution images. Therefore, using a numerical integration scheme [52], Eq. (31) is rewritten in light-cone coordinates:

$$\mu = t - r_*, \qquad \nu = t + r_*, \tag{34}$$

yielding

$$\frac{\partial^2 \Psi}{\partial u \partial v} + \frac{1}{4}V(r)\Psi = 0, \tag{35}$$

where $\Psi(u,v) \to \Psi_{ij}$ and

$$\frac{\partial \Psi}{\partial u} \to \frac{\Psi_{i+1,j} - \Psi_{i-1,j}}{\triangle u}, \tag{36}$$

$$\frac{\partial \Psi}{\partial v} \to \frac{\Psi_{i,j+1} - \Psi_{i,j-1}}{\triangle v}.$$

Using the central difference rule,

$$\Psi_{i,j} = \frac{\Psi_W + \Psi_E}{2}, \tag{37}$$

we get a discrete expression for Eq. (35)

$$\Psi_N = \Psi_W + \Psi_E - \Psi_S - \triangle u \triangle v V(r) \frac{\Psi_W + \Psi_E}{8}. \tag{38}$$

The notations we use here are

$$\Psi_N = \Psi_{i+1,j+1}, \Psi_S = \Psi_{i-1,j-1}, \tag{39}$$
$$\Psi_E = \Psi_{i+1,j-1}, \Psi_W = \Psi_{i-1,j+1}.$$

We adopt the finite difference method to analyse the stability of Einstein-Gauss-Bonnet BHs in AdS space-time with $\Lambda = -\frac{n(n-1)}{2r_h^2}$ and $r_h = 1$. The temporal evolution of various modes in Fig. 3 is consistent with each situation in Fig. 2.

From Fig. 3(a) - (c), the Gauss-Bonnet coupling parameter α in 5-dimensional ($n = 3$) AdS spacetime is analyzed. Figure 3 shows the detailed evolution of gravitational perturbation fields (including tensor, vector, and scalar types) in higher dimensional Einstein-Gauss-Bonnet AdS spacetime. In all types of gravitational perturbations, the QNMs of Einstein-Gauss-Bonnet BHs with $\alpha \leq 0.3$ tend to oscillate stably. Even if α increases exponentially, damping become dominant. In Fig. 2(b) and Fig. 2(c) the vector and scalar types of perturbation respectively have negative regions, which probably does not lead to instability, but the quasinormal ringing is suppressed by this negative region, cf. Fig. 3(b) and Fig. 3(c). Hence, it causes the QNM ringing period to disappear after the initial disturbance.

We show that stable typical damped ($\alpha \leq 0.3$) and evolving time domain picture of the instability near the critical value in Fig. 3(a) - (c). Note that when α increases to a certain critical value, the instability of QNMs in Einstein-Gauss-Bonnet AdS spacetime occurs. The dynamic evolution of tensor, vector, and scalar perturbations becomes unstable when $\alpha = 0.45$, 0.5, and 0.35 respectively. That means that the stronger Gauss-Bonnet coupling parameter α leads to slower decay of the perturbations, which will further cause instability of the Einstein-Gauss-Bonnet BH. Therefore, we show that the parametric region of the BHs is stable but shows the beginning of instability. Additionally, we can see the Einstein-Gauss-Bonnet AdS BH remains stable when $\alpha = 0.01$. Therefore, we calculate the QNMs of gravitational perturbations with $\alpha = 0.01$, to distinguish the Einstein-Gauss-Bonnet BHs and classics BHs of QNMs.

Figure 3(d) - (f) shows the stability of Einstein-Gauss-Bonnet BHs in different higher dimensional AdS spacetimes with $\alpha = 0.01$ and $l = 2$. Moreover, when a $\alpha \rightarrow 0$, an Einstein-Gauss-Bonnet BH becomes a higher-dimensional Schwarzschild-Tangherlini spacetime, which returns to a classical Schwarzschild BH with $n = 2$ and

$\alpha = 0$. $\mathrm{Re}(\omega)$ and $|\mathrm{Im}(\omega)|$ both increase as n increases, which indicates that $\mathrm{Re}(\omega)$ becomes much more intense than a Schwarzschild BH ($n = 2$ and $\alpha = 0$), and the decay rate $|\mathrm{Im}(\omega)|$ is faster than that of a Schwarzschild BH.

Figure 3(g) - (i) shows the stability of Einstein-Gauss-Bonnet BHs in 5-dimensional ($n = 3$) AdS spacetime with $\alpha = 0.01$. As the angular quantum number l increases, $\mathrm{Re}(\omega)$ increases significantly, while the decay rate ($|\mathrm{Im}(\omega)|$) decreases.

4.2   Numerical calculation

We use the discretization scheme proposed by Gary T. Horowitz and Veronika E. Hubeny [52, 53] to study the QNMs in Einstein-Gauss-Bonnet AdS spacetime. Therefore, in the ingoing Eddington coordinates, Eq. (31) should be reformulated with $v = t + r_*$:

$$f(r)\frac{\partial^2 \Psi}{\partial r^2} + [f'(r) - 2i\omega]\frac{\partial \Psi}{\partial r} - \widetilde{V}(r)\Psi = 0, \tag{40}$$

where $\Psi(r) = \mathrm{e}^{i\omega r}\Phi(r)$ and $\widetilde{V}(r) = \frac{V(r)}{f(r)}$. $x = 1/r$ is introduced to the region outside BH, defining $x_+ = 1/r_+$. Equation (40) is expressed as

$$s(x)\frac{\mathrm{d}^2 \Psi}{\mathrm{d}x^2} + \frac{t(x)}{x - x_+}\frac{\mathrm{d}\Psi}{\mathrm{d}x} + \frac{u(x)}{(x - x_+)^2}\Psi = 0, \tag{41}$$

where

$$s(x) = -\frac{f(r)x^4}{x - x_+}, \tag{42}$$
$$t(x) = x^2[f(r)' - 2f(r)x - 2i\omega],$$
$$u(x) = (x - x_+)\widetilde{V}(r).$$

Around horizon r_h, $s(x)$, $t(x)$ and $u(x)$ can be expanded as

$$s(x) = \sum_{m=0}^{4} s_m(x - x_+)^m, \tag{43}$$
$$t(x) = \sum_{m=0}^{4} t_m(x - x_+)^m,$$
$$u(x) = \sum_{m=0}^{4} u_m(x - x_+)^m,$$

where $s_0 = 2x_+^2\kappa$, $t_0 = 2x_+^2(\kappa - i\omega)$ and $u_0 = 0$ ($\kappa = f'(r_h)/2$ represents the surface gravity of the BH). The wave function is $\Psi \sim (x - x_+)^\beta$ and Eq. (41) yields

$$\beta(\beta - 1)s_0 + \beta t_0 = 2x_+^2\beta(\beta\kappa - i\omega) = 0. \tag{44}$$

Accordingly, $\beta = 0$ represents ingoing modes in the AdS horizon. Then $\Psi \sim (x - x_+)^0$ is the approximate solution of the wave function around the horizon. Therefore we define

$$\Psi = \sum_{m=0}^{\infty} a_m(x - x_+)^m. \tag{45}$$

(a) Tensor perturbations: $n=3$, $l=2$ and $r_{\rm h}=1$

(b) Vector perturbations: $n=3$, $l=2$ and $r_{\rm h}=1$

(c) Scalar perturbations: $n=3$, $l=2$ and $r_{\rm h}=1$

(d) Tensor perturbations: $l=2$, $\alpha=0.01$ and $r_{\rm h}=1$

(e) Vector perturbations: $l=2$, $\alpha=0.01$ and $r_{\rm h}=1$

(f) Scalar perturbations: $l=2$, $\alpha=0.01$ and $r_{\rm h}=1$

(g) Tensor perturbations: $n=3$, $\alpha=0.01$ and $r_{\rm h}=1$

(h) Vector perturbations: $n=3$, $\alpha=0.01$ and $r_{\rm h}=1$

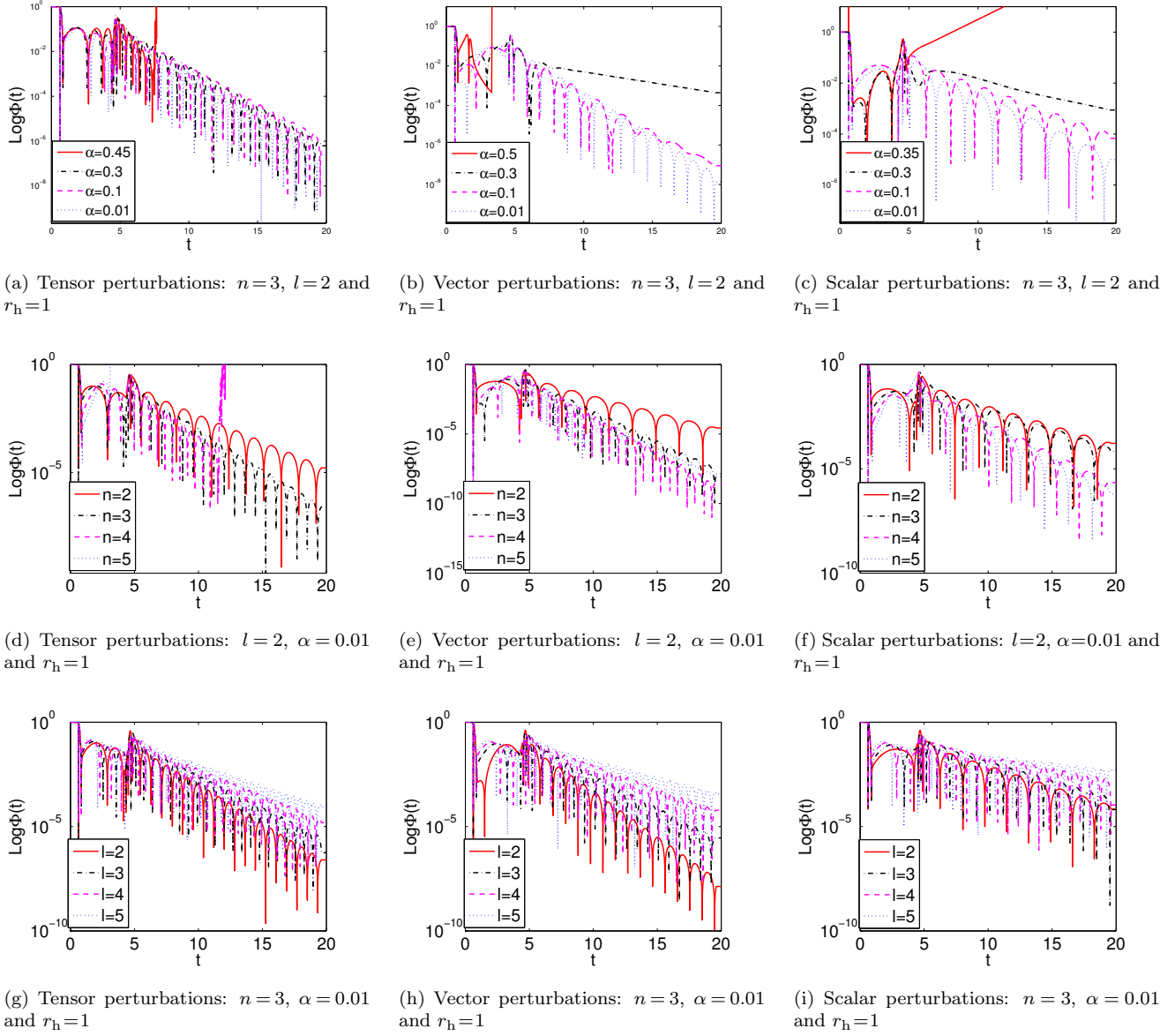(i) Scalar perturbations: $n=3$, $\alpha=0.01$ and $r_{\rm h}=1$

Fig. 3.   (color online) The dynamical evolution for all types of gravitational perturbations in Einstein-Gauss-Bonnet AdS spacetime ($\Lambda=-\frac{n(n-1)}{2r_{\rm h}^2}$ and $r_{\rm h}=1$) with different values of α, n, and l: (a), (d) and (g) are for the tensor type; (b), (e) and (h) are for the vector type; and (c), (f) and (i) are for the scalar type.

Substituting Eq. (43) and Eq. (45) into Eq. (44), the recurrence formula of a_m can be derived as [69]

$$a_m=-\frac{1}{m(m-1)s_0+mt_0}\Sigma_{j=0}^{\infty}a_j[j(j{-}1)s_{m-j}+jt_{m-j}+u_{m-j}], \tag{46}$$

here setting $a_0=1$. Using another boundary condition at $r\to\infty(x\to0)$, $\Psi\to0$, yields

$$\sum_{m=0}^{\infty}a_m(-x_+)^m=0. \tag{47}$$

Taking Eqs. (25) and (26) into the above equation, the algebraic equation of ω is solved by the iterative method.

The fundamental QNMs for the three types of gravitational perturbation, calculated by the Horowitz and Hubeny method, are given in Tables 1, 2 and 3. We mainly focus on the effect of α in the different dimensions. The results show that α would increase the frequency of oscillation $\mathrm{Re}(\omega)$ (n is held constant), but would decrease the decay rate $|\mathrm{Im}(\omega)|$ except the case of $n=2$. Since $n=2$ for a Einstein-Gauss-Bonnet AdS

Table 1.   Tensor gravitational perturbations for Einstein-Gauss-Bonnet AdS BHs, $r_{\rm h}=1$, $l=2$, $\Lambda=-\frac{n(n-1)}{2r_{\rm h}^2}$.

α	$n=2$	$n=3$	$n=4$
0.1	$2.34096555-0.42801937i$	$6.92285542-0.612430224i$	$8.35573638-1.07776817i$
0.01	$2.34096555-0.42801937i$	$6.69814978-0.614303907i$	$8.15232034-1.08129254i$
0.001	$2.34096555-0.42801937i$	$6.69590424-0.637235403i$	$8.09896332-1.08175591i$
0.0001	$2.34096555-0.42801937i$	$6.69547613-0.639571231i$	$8.09436918-1.08263107i$

Table 2.   Vector gravitational perturbations for Einstein-Gauss-Bonnet AdS BHs, $r_{\rm h}=1$, $l=2$, $\Lambda=-\frac{n(n-1)}{2r_{\rm h}^2}$.

α	$n=2$	$n=3$	$n=4$
0.1	$1.71539459-0.549173291i$	$3.30910851-0.544646153i$	$4.55613638-0.87652084i$
0.01	$1.71539459-0.549173291i$	$3.25540325-0.562397563i$	$4.35573638-0.95566896i$
0.001	$1.71539459-0.549173291i$	$3.21429942-0.567733641i$	$4.33661026-1.05033999i$
0.0001	$1.71539459-0.549173291i$	$3.20749423-0.568562154i$	$4.33260148-1.05594466i$

Table 3.   Scalar gravitational perturbations for Einstein-Gauss-Bonnet AdS BHs, $r_{\rm h}=1$, $l=2$, $\Lambda=-\frac{n(n-1)}{2r_{\rm h}^2}$.

α	$n=2$	$n=3$	$n=4$
0.1	$1.69656429-0.42529586i$	$1.99326015-0.35548921i$	$13.7557363-0.55566893i$
0.01	$1.69656429-0.42529586i$	$1.98294621-0.48272505i$	$13.5126658-0.60197929i$
0.001	$1.69656429-0.42529586i$	$1.91962459-0.49008132i$	$13.4005969-0.60538738i$
0.0001	$1.69656429-0.42529586i$	$1.91225165-0.49109236i$	$13.3755785-0.60780494i$

BH, like a classical Schwarzschild AdS BH, the Gauss-Bonnet coupling parameter α is trivial. Moreover, we see that $\text{Re}(\omega)$ and $|\text{Im}(\omega)|$ both increase as dimension n increases, for a given α.

5   Conclusion

In this paper, we studied the spherically symmetric solution representing a static BH in asymptotically flat, dS, and AdS spacetimes. Then the QNMs of gravitational perturbations in AdS spacetimes were investigated. It is noteworthy that around $r \to \infty$ in AdS spacetime is different from the situations in flat and dS spacetimes [70, 71]. The potential $\widetilde{V}(r)$ of the master equation at infinity does not tend to zero but to infinity in AdS spacetime. The main focus of the paper is, therefore, to analyze the dynamic evolution of the Einstein-Gauss-Bonnet BH according to the finite difference method in AdS spacetimes, varying the value of α, the dimensionality of spacetime n, and the multipole numbers l. Finally, the QNMs of gravitational perturbations of Einstein-Gauss-Bonnet BHs in AdS spacetimes were calculated by the Horowitz and Hubeny method.

Using the finite difference method, we find that perturbation frequency $\text{Re}(\omega)$ increases but the decay rate $|\text{Im}(\omega)|$ decreases with increasing α. More remarkably, we have found that vector and scalar perturbations have a negative gap which probably does not cause instability but suppresses the quasinormal ringing to be an exponential tail. Therefore, we are unable to see the QNM ringing period after the initial outburst. Nevertheless, when α increases to some critical value ($\alpha=$ 0.45,0.5,0.35 respectively), instability of the QNMs occurs in Einstein-Gauss-Bonnet AdS spacetime. In accordance with the AdS/CFT correspondence, instability of the QNMs possibly forecasts limits of holographic applicability in Einstein-Gauss-Bonnet AdS backgrounds. As we increase n, perturbation frequency $\text{Re}(\omega)$ and decay rate $|\text{Im}(\omega)|$ both increase. Meanwhile, $\text{Re}(\omega)$ increases and the decay rate $|\text{Im}(\omega)|$ decreases when the angular quantum number l increases. The results of QNMs from the Horowitz and Hubeny method are consistent with the above properties of Gauss-Bonnet AdS BHs.

As a summary, we can draw the following conclusions. (i) The existence of α can affect the QNMs of Einstein-Gauss-Bonnet AdS BHs. When α approaches 1, as forecast by string theory, some different properties from Einstein-Gauss-Bonnet AdS BH QNMs of gravitational perturbations will appear. When TeV-scale quantum gravity scenarios are taken into account, the effects of α on the QNM spectrum should not be ignored The result of the finite difference method indicates that Einstein-Gauss-Bonnet AdS BHs become more and more unstable at larger α. Einstein-Gauss-Bonnet theory comes from a one-loop string theory approximation, which is valid when α is small. (ii) In the higher dimensional spacetimes, the decay rate of $|\text{Im}(\omega)|$ decreases with the increase of α and n, which is connected with the mass of Einstein-Gauss-Bonnet AdS BHs. In the matter of AdS/CFT correspondence, this signifies that the greater the mass, the more time the Einstein-Gauss-Bonnet BH takes to approach equilibrium. Therefore, in this study the results we obtained not only contribute α for QNMs of Einstein-Gauss-Bonnet AdS BHs, but also

provide useful reference information for research into AdS/CFT correspondence.

We are indebted to Dr. Hao Wen for help.

References

1   B. Zwiebach, Phys. Lett. B, **156**: 315 (1985)
2   J. T. Wheeler, Nucl. Phys. B, **273**: 732 (1986)
3   D. L. Wiltshire, Phys. Rev. D, **38**: 2445 (1988)
4   T. Thiemann Lect, Notes. Phys., **41**: 631 (2003)
5   L. Randall and R. Sundrum, Phys. Rev. Lett., **83**: 4690 (1999)
6   Ashoke Sen, J. High. Energy. Phys., **0603**: 008 (2006)
7   F. Moura and R. Schiappa, Class. Quantum Grav., **24**: 361 (2007)
8   D. J. Gross and E. Witten, Nucl. Phys. B, **277**: 1 (1986)
9   J. Scherk and J. H. Schwarz, Nucl. Phys. B, **81**: 118 (1974)
10 N. Deppe, C. D. Leonard, T. Taves, G. Kunstatter, and R. B. Mann, Phys. Rev. D, **86**: 104011 (2012)
11 S. Golod and T. Piran, Phys. Rev. D, **85**: 104015 (2012)
12 D. G. Boulware, and S. Deser, Phys. Rev. Lett., **55**: 2656 (1985)
13 A. Barrau, J. Grain, and S. O. Alexeyev, Phys. Lett. B, **584**: 114 (2004)
14 D. G. Boulware and S. Deser, Phys. Rev. Lett., **55**: 2656 (1985)
15 J. T. Wheeler, Nucl. Phys. B, **268**: 737 (1986)
16 R. Konoplya, Phys. Rev. D, **71**: 024038 (2005)
17 E. Abdalla, R. A. Konoplya, and C. Molina, Phys. Rev. D, **72**: 084006 (2005)
18 M. A. Cuyubamba, R. A. Konoplya, and A. Zhidenko, Phys. Rev. D, **93**: 104053 (2016)
19 R. A. Konoplya and A. Zhidenko Rev. Mod. Phys., **83**: 793 (2011)
20 R. A. Konoplya, Phys. Rev. D, **82**: 084003 (2010)
21 R. A. Konoplya, Phys. Rev. Lett., **103**: 161101 (2009)
22 G. Dotti and R. J. Gleiser, Phys. Rev. D, **72**: 044018 (2005)
23 R. J. Gleiser and G. Dotti, Phys. Rev. D, **72**: 124002 (2005)
24 R. A. Konoplya, Phys. Rev. D, **77**: 104004 (2008)
25 E. Berti, V. Cardoso, and A. O. Starinets, Class. Quant. Grav., **26**: 163001 (2009)
26 C. V. Vishveshwara, Phys. Rev. D , **1**: 2870 (1970)
27 E. Berti, V. Cardoso, and C. M. Will, Phys. Rev. D, **73**: 064030 (2006)
28 K. D. Kokkotas and B. G. Schmidt, Living Rev. Relativity 2, 2 (1999)
29 C. Gundlach, R. H. Price, and J. Pullin, Phys. Rev. D, **49**: 883 (1994)
30 H. Shahar, Phys. Rev. Lett., **81**: 4293 (1998)
31 Olaf Dreyer, Phys. Rev. Lett., **90**: 081301 (2003)
32 L. Motl and Adv. Neitzke Theor. Math. Phys., **7**: 307 (2003)
33 E. Berti and K. D. Kokkotas, Phys. Rev. D, **67**: 064020 (2003)
34 B. P. Abbott et al, Phys. Rev. Lett., **116**: 241103 (2016)
35 B. P. Abbott et al, Phys. Rev. Lett., **116**: 061102 (2016)
36 B. P. Abbott et al, Phys. Rev. Lett., **118**: 221101 (2017)
37 B. P. Abbott et al, Phys. Rev. Lett., **119**: 161101 (2017)
38 R. Konoplya and A. Zhidenko, Phys. Lett. B, **756**: 350 (2016)
39 J. Maldacena, Adv. Theor. Math. Phys., **2**: 253 (1998)
40 E. Witten, Adv. Theor. Math. Phys., **2**: 253 (1998)
41 O. Lunin, S. Mathur, Nucl. Phys. B, **623**: 342 (2002)
42 V. Cardoso, José P S Lemos, Phys. Rev. D, **64**: 084017 (2001)
43 A. Nunez and A. O. Starinets, Phys. Rev. D, **67**: 124013 (2003)
44 M. Maliborski and A. Rostworowski, Phys. Rev. Lett., **111**: 051102 (2013)
45 A. Buchel, S. L. Liebling, and L. Lehner, Phys. Rev. D, **87**: 123006 (2013)
46 P. Bizoń and J. Jałmużna, Phys. Rev. Lett., **111**: 041102 (2013)
47 A. Buchel, L. Lehner, and S. L. Liebling, Phys.Rev. D, **86**: 123011 (2012)
48 D. Santos Oliván and F. Sopuerta Carlos, Phys. Rev. Lett., **116**: 041101 (2016)
49 K. Lin, W. L. Qian and A. B. Pavan, Phys. Rev. D, **94**: 064050 (2016)
50 H. Ma and J, Li, Chin. Phys. B, **26**: 060400 (2017).
51 C. Gundlach, H. P. Richard, and J. Pullin, Phys. Rev. D, **49**: 890 (1994)
52 G. T. Horowitz and V. E. Hubeny, Phys. Rev. D, **62**: 024027 (2000)
53 G. T. Horowitz, Class. Quantum Grav. D, **17**: 1107 (2000)
54 D. Lovelock, J. Math. Phys., **12**: 498 (1971)
55 M. H. Dehghani and R. Pourhasan, Phys. Rev. D, **79**: 064015 (2009)
56 C. Teitelboim and J. Zanelli, Class. and Quant. Grav., **4**: L125 (1987)
57 M. Banados, C. Teitelboim, and J. Zanelli, Phys. Rev. D, **49**: 975 (1994)
58 M. Banados, C. Teitelboim, and J. Zanelli, Phys. Rev. D, **49**: 986 (1994)
59 R. G. Cai, Phys. Rev. D, **65**: 084014 (2002)
60 F. R. Tangherlini, Nuovo Cim., **27**: 636 (1963)
61 J. Li, K. Lin, H. Wen, and W. Liang Qian, Advances in High Energy Physics 2017, 19 (2017)
62 T. Takahashi, and J. Soda, Prog. Theor. Phys., **124**: 911 (2010)
63 B. Schutz and C. M. Will, Astrophys. J., **291**: L33 (1988)
64 S. Iyer and C. M. Will, Phys. Rev D, **35**: 3621 (1985)
65 V. Ferrari and B. Mashhoon, Phys. Rev. D, **30**: 295 (1984)
66 N. Andersson and S. Linnaeus, Phys. Rev. D, **46**: 4179 (1992)
67 E. W. Leaver, Proc. R. Soc. A, **402**: 285 (1985)
68 R. A. Konoplya and A. Zhidenko, Nucl. Phys. B, **777**: 182 (2007)
69 B. Wang, C.Y. Lin, and E. Abdalla, Phys. Lett. B, **481**: 79 (2000)
70 S. S. Gubser, I. R. Klebanov, and A. M. Polyakov, Phys. Lett. B, **428**: 105 (1998)
71 O. Aharony, S.S. Gubser, J. Maldacena, H. Ooguri, and Y. Oz, Phys. Rept., **323**: 183 (2000)